The Astrophysical Journal, 628:388–394, 2005 July 20

ORBITAL X-RAY VARIABILITY OF THE MICROQUASAR LS 5039

Valentí Bosch-Ramon,[1] Josep M. Paredes,[1] Marc Ribó,[2] Jon M. Miller,[3,4] Pablo Reig,[5,6] and Josep Martí[7]

Received 2004 October 14; accepted 2005 February 26

ABSTRACT

The properties of the orbit and the donor star in the high-mass X-ray binary microquasar LS 5039 indicate that accretion processes should mainly occur via a radiatively driven wind. In such a scenario, significant X-ray variability would be expected due to the eccentricity of the orbit. The source has been observed at X-rays by several missions, although with a poor coverage that prevents reaching any conclusion about orbital variability. Therefore, we conducted *RXTE* observations of the microquasar system LS 5039 covering a full orbital period of 4 days. Individual observations are well fitted with an absorbed power law plus a Gaussian at 6.7 keV, to account for iron-line emission that is probably a diffuse background feature. In addition, we have taken into account that the continuum is also affected by significant diffuse background contamination. Our results show moderate power-law flux variations on timescales of days, as well as the presence of miniflares on shorter timescales. The new orbital ephemerides of the system recently obtained by Casares et al. have allowed us to show, for the first time, that an increase of emission is seen close to the periastron passage, as expected in an accretion scenario. Moreover, the detected orbital variability is a factor of $\sim$4 smaller than the one expected by using a simple wind accretion model, and we suggest that an accretion disk around the compact object could be responsible for this discrepancy. On the other hand, significant changes in the photon index are also observed, clearly anticorrelated with the flux variations. We interpret the overall X-ray spectral characteristics of LS 5039 in the context of X-ray radiation produced by inverse Compton and/or synchrotron processes in the jet of this microquasar.

Subject headings: accretion, accretion disks — binaries: close — stars: individual (LS 5039) — X-rays: binaries — X-rays: individual (RX J1826.2−1450)

1. INTRODUCTION

LS 5039/RX J1826.2−1450 is a high-mass X-ray binary runaway microquasar at a distance of $\sim$2.9 kpc from the Earth (Paredes et al. 2000; Ribó et al. 2002). Paredes et al. (2000) proposed that this microquasar is the counterpart of the high-energy γ-ray source 3EG J1824−1514 (Hartman et al. 1999) and suggested that microquasars could be the counterparts of some of the unidentified Energetic Gamma-Ray Experiment Telescope (EGRET) sources. In addition, Torres et al. (2001) classified this source as variable, and Bosch-Ramon & Paredes (2004) have proposed a model based on an inhomogeneous jet, emitting at γ-rays via inverse Compton scattering, giving theoretical support to the possible association between the microquasar and the EGRET source.

The first radio detection was reported by Martí et al. (1998) using the Very Large Array (VLA), but the discovery of the radio jets was only possible when the source was observed at milliarcsecond scales with the Very Long Baseline Array (VLBA; Paredes et al. 2000). The presence of an asymmetric and persistent radio jet has been confirmed with new Multielement Radio-linked Interferometer Network (MERLIN) and European VLBI Network (EVN) observations (Paredes et al. 2002). The radio emission is persistent, nonthermal, and variable, although no strong radio outbursts or periodic variability have been detected so far (Ribó et al. 1999; Ribó 2002).

In the optical band, LS 5039 appears as a bright $V = 11.2$, O6.5 V((f)) star showing little variability on timescales of months to years (Clark et al. 2001). Variations of $\sim$0.4 mag have been reported in the infrared (H and K bands), but no obvious mechanisms for such variability have been proposed (Clark et al. 2001). Using the radial velocities reported in McSwain et al. (2001, 2004) and newly obtained ones, Casares et al. (2005) have determined the most recent values for the orbital period and the eccentricity for this binary system, $P_{\rm orb} = 3.9060 \pm 0.0002$ days (with $t_0 = \mathrm{HJD}\ 2{,}451{,}943.09 \pm 0.10$) and $e = 0.35 \pm 0.04$, respectively, with the periastron passage at phase 0.0.

In the X-ray domain the source has been observed several times using different satellites, presenting fluxes spanning 1 order of magnitude in the range $\sim(5-50) \times 10^{-12}$ ergs cm^{-2} s^{-1} (see § 2). These fluxes imply luminosities in the range $\sim(0.5-5) \times 10^{34}$ ergs s^{-1}, assuming a distance of 2.9 kpc. Variations in the photon index have also been observed. So far, it has been unclear whether these variations in flux and spectral slope were related to long-term variations in the mass-loss rate of the companion or to accretion changes along the eccentric orbit.

To determine the possible flux and photon index variations along a whole orbital period, we proposed X-ray observations of LS 5039 to be performed with the *Rossi X-Ray Timing Explorer* (*RXTE*) satellite during four consecutive days in 2003 July. Photometric and spectroscopic optical observations were performed

[1] Departament d'Astronomia i Meteorologia, Universitat de Barcelona, Avenida Diagonal 647, 08028 Barcelona, Spain; vbosch@am.ub.es; jmparedes@ ub.edu.
[2] Service d'Astrophysique, Commissariat à l'Énergie Atomique (CEA) de Saclay, Bâtiment 709, L'Orme des Merisiers, 91191 Gif-sur-Yvette Cedex; and AIM, Unité Mixte de Recherche, CEA, CNRS, Université Paris VII, UMR No. 7158, Paris, France; mribo@discovery.saclay.cea.fr.
[3] Harvard-Smithsonian Center for Astrophysics, 60 Garden Street, Cambridge, MA 02138; jmmiller@head-cfa.harvard.edu.
[4] National Science Foundation Astronomy and Astrophysics Postdoctoral Fellow.
[5] Grupo de Astronomía y Ciencias del Espacio, Instituto de Ciencias de los Materiales, Universitat de València, 46071 Paterna-València, Spain; pablo.reig@ uv.es.
[6] Institute of Electronic Structure and Laser, Foundation for Research and Technology—Hellas; and Physics Department, University of Crete, P.O. Box 208, 71003 Heraklion, Greece; pau@physics.uoc.gr.
[7] Departamento de Física, Escuela Politécnica Superior, Universidad de Jaén, Virgen de la Cabeza 2, 23071 Jaén, Spain; jmarti@ujaen.es.

TABLE 1
SUMMARY OF PREVIOUS X-RAY OBSERVATIONS

Date	Mission	Phase	Photon Index	Extrapolated 3–30 keV Flux (10^{-11} ergs cm^{-2} s^{-1})
1998 Feb 8	*RXTE*	0.803–0.837	1.95 ± 0.02	5.6
1998 Feb 8	*RXTE*	0.006–0.057	1.95 ± 0.02	4.6
1998 Feb 16	*RXTE*	0.039–0.059	1.95 ± 0.02	4.6
1999 Oct 4	*ASCA*	0.382–0.471	~ 1.6	2.7
2000 Oct 8	*BeppoSAX*	0.969–0.205	1.8 ± 0.2	0.8
2002 Sep 10	*Chandra*	0.690–0.720	1.14 ± 0.20	2.3
2003 Mar 8	*XMM-Newton*	0.526–0.557	$1.56^{+0.02}_{-0.05}$	2.0
2003 Mar 27	*XMM-Newton*	0.533–0.564	$1.49^{+0.05}_{-0.04}$	2.0

NOTE.—Errors are within the 90% confidence level.

simultaneously with the X-ray ones. Regarding the photometry, Martí et al. (2004) have reported that no photometric variability above ± 0.01 mag took place during six consecutive nights. Regarding the spectroscopy, Casares et al. (2005) have found a nearly constant equivalent width of the Hα absorption line of EW $\sim$ 2.8 Å, implying no significant changes in the mass-loss rate of the primary during our *RXTE* observations.

This work has been organized as follows. In § 2, we present results from previous X-ray observations. In § 3, we show the results obtained from our *RXTE* data reduction and analysis. Furthermore, in § 4, we discuss our results in the context of both previous observations and the microquasar scenario, and finally, in § 5, we summarize this work.

2. PREVIOUS X-RAY RESULTS

The first X-ray detection of LS 5039/RX J1826.2−1450 was made with the *Röntgensatellit* (*ROSAT*) in 1996 October, obtaining a flux of 7.1×10^{-12} ergs cm^{-2} s^{-1} in the range 0.1–2.4 keV (Motch et al. 1997). Ribó et al. (1999) reported *RXTE* observations carried out on 1998 February 8 and 16. The flux detected in the energy range 3–30 keV was $\sim 50 \times 10^{-12}$ ergs cm^{-2} s^{-1}, and the obtained photon index was $\Gamma = 1.95$, although these values are likely affected by contamination from the diffuse background (see discussion in § 3.2). The X-ray timing analysis indicated the absence of pulsed or periodic emission on timescales of 0.02–2000 s. The source spectrum was well represented by a power-law model plus a Gaussian component describing a strong iron line at 6.7 keV. Significant emission was seen up to 30 keV, and no exponential cutoff at high energy was required. Unpublished observations performed by the *Advanced Satellite for Cosmology and Astrophysics* (*ASCA*; 1999 October 4) present a photon index of about 1.6 and an unabsorbed flux in the range 0.3–10 keV of about 13×10^{-12} ergs cm^{-2} s^{-1} (Martocchia et al. 2005). *BeppoSAX* observations, on 2000 October 8, found a flux of $\sim 5 \times 10^{-12}$ ergs cm^{-2} s^{-1} (0.3–10 keV), a photon index of 1.8, and a hydrogen column density of $N_{\rm H} = 1.0^{+0.4}_{-0.3}$ cm^{-2} (Reig et al. 2003b). These authors also concluded that an X-ray eclipse by the companion star was ruled out by these data. The new ephemerides obtained by Casares et al. (2005) confirm that the *BeppoSAX* observations took place during the inferior conjunction of the primary. The lack of eclipses provides an upper limit for the inclination of the system of $i < 69^\circ \pm 1^\circ$ (see discussion in Reig et al. 2003b for details). We have analyzed unpublished *Chandra* data (2002 September 10) and have found a flux of 8.9×10^{-12} ergs cm^{-2} s^{-1} and $\Gamma = 1.14 \pm 0.12$ in the range 0.3–10 keV. Finally, *XMM-Newton* observations of LS 5039 were carried out recently (2003 March 8 and 27) and showed that the source presented a flux of about 10×10^{-12} ergs cm^{-2} s^{-1} (0.3–10 keV) and a photon index of about 1.5 (Martocchia et al. 2005). Very similar fluxes and photon indexes are found for both observing periods, consistent with the fact that both were taken at the same orbital phase (around 0.55 with the new ephemerides).

In any but the *RXTE* observations in 1998, a Gaussian component in addition to the absorbed power-law model does not improve the fit. Therefore, it is possible that the Gaussian line of the 1998 *RXTE* observations could come from the Galactic ridge, being present because of the large field of view and effective area of the instrument. We investigate this issue below. For all the observations, disk features are not necessary to fit the data.

We list in Table 1 the dates, missions, orbital phases, photon indexes, and extrapolated fluxes in the energy range 3–30 keV of LS 5039 using a power-law spectrum, assuming the same slope up to 30 keV, for all the prior observations but the *ROSAT* one (because of the big difference in energy range). Although it is clear that photon index and flux changes are present, since the different observations are separated by months/years in time, it has not been possible up to now to clearly establish whether the intensity of the emission changed with time due to variations in the mass-loss rate of the stellar companion or due to the orbital eccentricity. There is observational evidence supporting the first option, based on correlations found between the wind intensity of the companion (inferred from the equivalent width of the Hα absorption line) and the observed X-ray flux (Reig et al. 2003b; McSwain et al. 2004), although this does not preclude the second one from occurring as well. The photon index variation could also be a consequence of either long-term phenomena, short-term phenomena, or both.

3. *RXTE* OBSERVATIONS

The main goal of these observations was to perform an in-depth study of the X-ray variability during a full orbital period of the microquasar LS 5039. In particular, we wanted to answer the following questions: Does the source flux vary with orbital phase due to a geometric effect related to the eccentricity of the binary system? Is the power-law index dependent on the orbital phase? Does the iron line come from the source? This section tries to answer these three queries, although a deeper and wider discussion is developed in § 4.

3.1. *Data Reduction and Analysis*

RXTE observed the source on 17 runs of different duration covering a total of 4 days between 2003 July 4 and 8. Due to the relatively faint emission of LS 5039 during the observations, the source spectrum is background dominated beyond 30 keV, so High-Energy X-Ray Timing Experiment (HEXTE) data have

TABLE 2
SUMMARY OF *RXTE* OBSERVATIONS

Middle Time (MJD)	Duration (days)	Phase	Photon Index	Unabsorbed 3–30 keV Flux (10^{-11} ergs cm^{-2} s^{-1})
52,824.61.....	0.24	0.782–0.842	$1.84^{+0.04}_{-0.04}$	$6.21^{+0.16}_{-0.16}$
52,824.92.....	0.02	0.888–0.894	$2.04^{+0.09}_{-0.09}$	$5.09^{+0.26}_{-0.29}$
52,824.99.....	0.01	0.907–0.910	$2.03^{+0.11}_{-0.11}$	$5.14^{+0.30}_{-0.41}$
52,825.06.....	0.01	0.924–0.926	$2.18^{+0.14}_{-0.13}$	$4.32^{+0.30}_{-0.41}$
52,825.18.....	0.05	0.950–0.963	$1.94^{+0.13}_{-0.12}$	$5.48^{+0.35}_{-0.52}$
52,825.60.....	0.24	0.034–0.095	$2.09^{+0.05}_{-0.04}$	$4.42^{+0.10}_{-0.14}$
52,825.98.....	0.01	0.159–0.162	$1.69^{+0.08}_{-0.08}$	$6.95^{+0.29}_{-0.40}$
52,826.04.....	0.02	0.176–0.181	$1.98^{+0.12}_{-0.12}$	$4.54^{+0.32}_{-0.60}$
52,826.17.....	0.05	0.202–0.217	$1.98^{+0.12}_{-0.12}$	$5.14^{+0.33}_{-0.38}$
52,826.69.....	0.17	0.321–0.364	$1.96^{+0.05}_{-0.05}$	$5.12^{+0.14}_{-0.23}$
52,826.96.....	0.02	0.411–0.415	$2.08^{+0.11}_{-0.10}$	$4.82^{+0.17}_{-0.44}$
52,827.03.....	0.01	0.429–0.431	$2.13^{+0.11}_{-0.10}$	$4.58^{+0.24}_{-0.43}$
52,827.12.....	0.08	0.445–0.465	$2.16^{+0.12}_{-0.11}$	$4.51^{+0.30}_{-0.36}$
52,827.57.....	0.24	0.539–0.600	$2.04^{+0.02}_{-0.05}$	$4.98^{+0.14}_{-0.15}$
52,827.95.....	0.01	0.663–0.667	$2.01^{+0.11}_{-0.10}$	$5.02^{+0.28}_{-0.36}$
52,828.01.....	0.02	0.680–0.685	$2.06^{+0.09}_{-0.09}$	$5.09^{+0.22}_{-0.38}$
52,828.18.....	0.02	0.724–0.728	$1.90^{+0.07}_{-0.08}$	$5.80^{+0.24}_{-0.24}$

NOTE.—Errors are within the 90% confidence level.

not been considered, and we have focused on the analysis of Proportional Counter Array (PCA) data. For the four longer runs, only PCU 2[8] data were available, whereas two and even three detectors were on during significant fractions of time of the other runs (PCUs 1, 3, and 4). All the observations performed with the PCA have been reduced and analyzed. A summary of the observations is shown in Table 2.

We have reduced the data using the HEAsoft FTOOLS package, version 5.3.1. The spectral analysis has been performed with XSPEC, version 11.3.1. To carry out the data reduction, we have created a filter file to avoid data taken with an elevation angle with respect to the horizon smaller than 10°, electron-contaminated data, data taken during the South Atlantic Anomaly passage, and data with an offset of the pointings bigger than $0^{\circ}.02$. We have accounted also for the detectors that were on during the observation.

For the 17 runs, we have tried to fit the spectra with an absorbed power law plus a Gaussian emission line and a disk blackbody component. For all of them either the difference between models with and without a blackbody component is insignificant, or the blackbody flux is consistent with being zero. Therefore, to estimate the photon index and the fluxes of both the continuum and the line, we have fitted the data only with an absorbed power law plus a Gaussian line around 6.7 keV with fixed zero width (due to the low spectral resolution of *RXTE*). Regarding absorption, we note that inhomogeneities in the velocity and/or spatial distribution of the stellar wind could produce a variable amount of hydrogen column density, as has been observed in other wind-fed accreting systems such as GX 301−2 (White & Swank 1984). Unfortunately, it is not possible to extract such information from our *RXTE* data of LS 5039 due to the faint emission of the source, the relatively low value of $N_{\rm H}$, and the low-energy threshold of our data at 3 keV. Therefore, we have assumed a constant hydrogen column density and fixed it to a value of 8.7×10^{21} cm^{-2} (resulting from the average between the one found by Reig et al. [2003b] using the *BeppoSAX* data and the one derived from the formula of Predehl & Schmitt [1995] applied to the quoted value for A_V by McSwain et al. [2004]). The spectrum and the fit to the data taken at phase 0.78–0.84, during a long-lasting maximum of emission, are presented in Figure 1. The aspects of the spectra and the fits obtained from the other observations are quite similar to the one shown here. The date, time, and orbital phase of the 17 runs with their power-law indexes and unabsorbed fluxes for the power-law component in the energy range 3–30 keV are presented in Table 2.

Due to the low source flux, the upper limits on the source variability within a given run are not very constraining. The derived limits depend on a number of factors, including the fitting functions used (power laws, Lorentzians, etc.) and the background subtraction (total background is about 30 counts s^{-1} PCU^{-1} in the 3–30 keV energy range). Fast Fourier transforms of the high time resolution data from all active PCUs were performed to create power density spectra (PDSs) in the 0.01–1000 Hz range. Given the faint nature of the source, all available energy channels were combined when making the PDSs, and the obtained

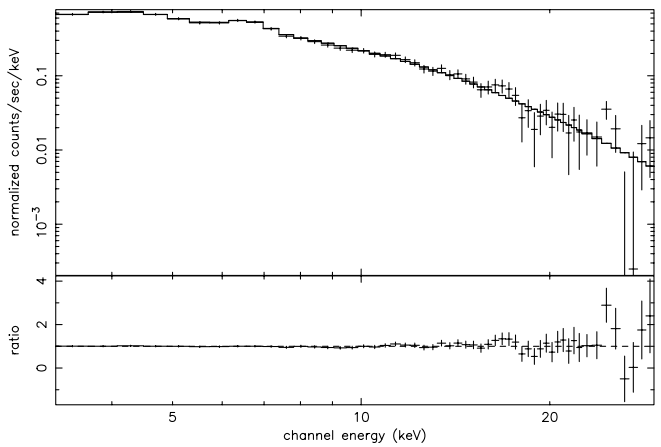

FIG. 1.—X-ray spectrum of LS 5039/RX J1826.2−1450 obtained with the data taken between phases 0.78 and 0.84. The solid line represents the fit to the data. The bottom panel shows the ratio between observed and fitted fluxes.

[8] Concerning PCU 0, despite efforts to recalibrate its response function following the loss of one of its gas layers, its spectra continue to deviate significantly at low energy compared to other PCUs. Therefore, although PCU 0 was also on during the runs, we have not included it in our spectral analysis.

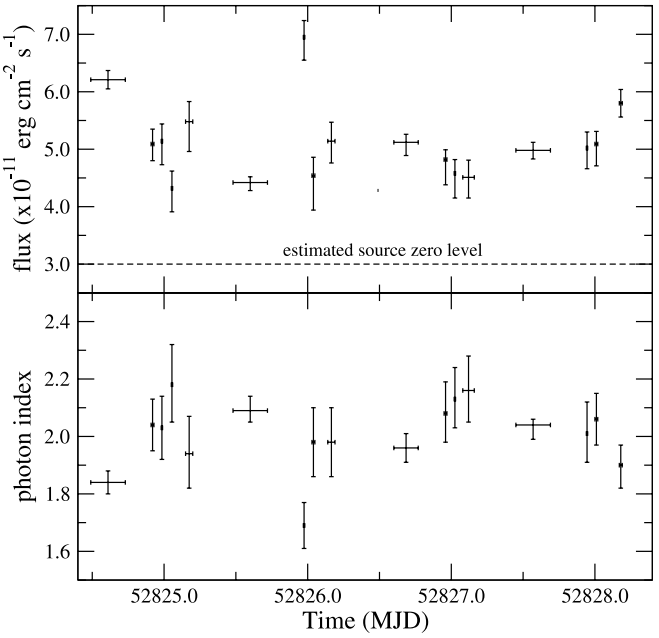

FIG. 2.—Unabsorbed power-law flux in the energy range 3–30 keV (*top panel*) and photon index (*bottom panel*) along the observational period, without subtracting the diffuse background model. The vertical error bars show the 90% confidence level, and the horizontal error bars show the duration of the observation in time. The estimated source zero level is indicated by a dashed line in the top panel.

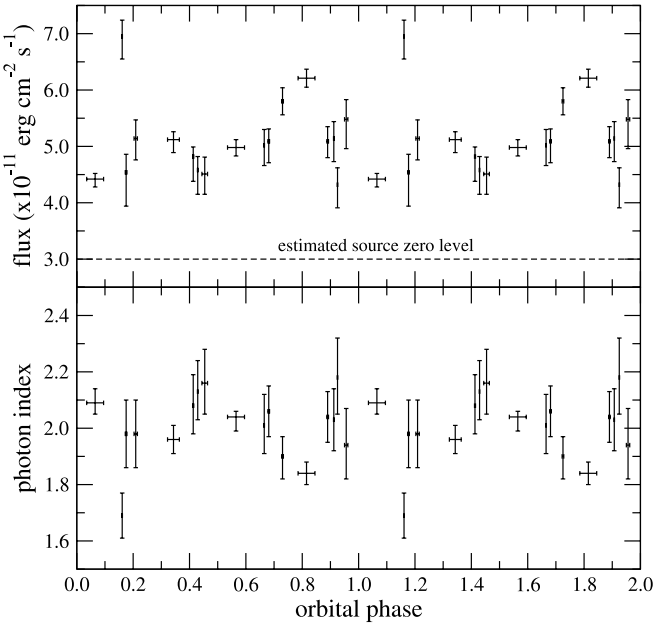

FIG. 3.—Same as Fig. 2, but as a function of the orbital phase, computed by using $P_{\rm orb} = 3.9060 \pm 0.0002$ days and $t_0 = \text{HJD } 2,451,943.09 \pm 0.10$. The periastron passage is at phase 0.0, and two orbital periods are shown for a better display.

fractional variability amplitude is generally less than 25% (3 σ). The PDSs are dominated by Poisson noise and generally appear to have no significant noise components that can be attributed to the source.

3.2. *Results*

The unabsorbed power-law flux and the photon index as a function of time are presented in Figure 2. We find evidence of day-to-day variations in both parameters. We show the same data folded with the orbital period in Figure 3. It can be seen that the flux appears to be moderately variable along the orbit, presenting a variation of 50% (see Table 2) with a long-lasting maximum at phase 0.8 and a short-duration maximum around phase 0.16. This short-duration maximum, of about half an hour, is more than 3 σ over the level of emission indicated by the adjacent points, and it is not unique, since other short-duration peaks are present even within the longer runs. The plotted flux in Figure 3 has been corrected for the internal background. However, this background-subtracted flux still contains a contribution from the diffuse background that is difficult to disentangle from the source spectrum and is estimated to be about 2 counts s^{-1} PCU^{-1}.[9] Applying an absorbed Raymond plus power-law model (see Valinia & Marshall 1998) to this count rate in the 3–30 keV energy interval, we obtain a diffuse background flux of about 3×10^{-11} ergs cm^{-2} s^{-1}. Thus, the ratio between the long-lasting maximum and the minimum fluxes after subtracting the diffuse background is $\sim$2.5.

In the bottom panel of Figure 3, we show the evolution of the photon index with the orbital phase. As can be seen, the photon index varies along the orbital period, presenting a hardening close to periastron. Actually, comparing in Figure 3 the unabsorbed power-law flux and the photon index evolutions at different phases of the orbit, an anticorrelation between both appears. This is better illustrated in Figure 4, where we plot the photon index as a function of the unabsorbed power-law flux. It seems that when the flux is higher, the photon index is harder, and the opposite happens when the flux is lower (this anticorrelation holds even within the longer observations when split and analyzed by parts). We stress here that changes in flux and photon index cannot be due to changes in the hydrogen column density for this weakly absorbed source, since we are working in the energy range 3–30 keV, or to diffuse background variations (internal background ones are already taken into account), since after applying the diffuse background model, the

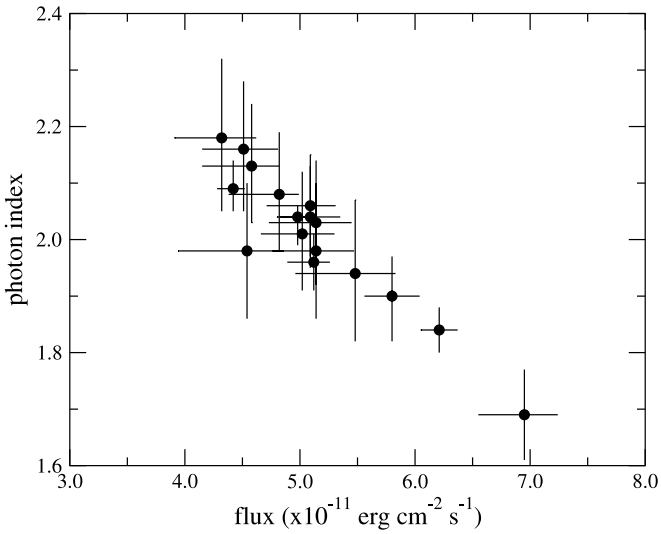

FIG. 4.—Photon index as a function of unabsorbed power-law flux in the energy range 3–30 keV, without subtracting the diffuse background model. The errors are within the 90% confidence level.

[9] Although this value has been found by the *RXTE* team after observations performed during the 2004 fall, we have assumed that during our observations, performed in 2003 July, it was roughly the same.

anticorrelation is still there. We note that the photon indexes calculated using this model are harder, in the range $\sim$1.3–1.6, more in accordance with those obtained in previous X-ray observations of the source, excluding the 1998 *RXTE* ones. Nevertheless, the uncertainty in the diffuse background model determination at the LS 5039 position requires one to be cautious about these results. Moreover, the flux variability does not seem to depend only on the photon index variability, since when fixing it to an intermediate value of 1.9 the flux variation is still significant. Another test has been done by fitting the unabsorbed flux data given in Table 2 with a constant value. The obtained reduced χ^2 greater than 3 indicates that the fit is not good. Moreover, the diffuse background cannot introduce variability, since its value, estimated by the *RXTE* team, remains constant within about 10% during periods of time longer than the orbital period. Finally, no significant optical variations have been observed in simultaneous photometric observations (Martí et al. 2004), which indicates that the companion star showed a stable behavior from the photometric point of view during our *RXTE* observations, reinforcing the idea that the measured X-ray flux variability is due to changes of the accretion rate in an eccentric orbit.

Although the data do not continuously cover the whole orbit, there appear to be two types of variation timescales in the light curves: one apparently linked to the orbital period of $\sim$3.9 days, and the other of shorter duration, like miniflares, of about 1 hr. No significant changes are detected through simultaneous (although not strictly) spectroscopic observations of the Hα line along the orbit on day timescales (Casares et al. 2005). Thus, stellar wind changes can be ruled out to explain the first type of variability. In contrast, fast fluctuations in the stellar wind might be related to the shorter timescale variability, as significant variations on timescales of minutes have been observed in radial velocity measurements of LS 5039 (see Fig. 2 of Casares et al. [2005], around HJD 2,452,827.7). Unfortunately, there is no spectroscopic data right before these miniflares observed in X-rays.

Our fits to the spectra are consistent with the presence of a line at 6.7 ± 0.1 keV in the data, as in the previous *RXTE* observations (Ribó et al. 1999). However, as mentioned above, no other X-ray mission but *RXTE* (which does not have imaging capabilities) reported the presence of the iron line, so its origin could be in the Galactic plane regions behind the source and due to the so-called Galactic ridge emission. One possible test for determining whether the line is related to LS 5039 would be the presence or lack of line-flux variations correlated with continuum flux changes. In fact, the different values of the line flux obtained on the different runs are always consistent, at 90% confidence, with their average value of $\sim 1.65 \times 10^{-4}$ photons cm^{-2} s^{-1} per PCU beam of 0.9 deg^2. For comparison, the value of the iron-line flux at the LS 5039 position after measurement with the *Ginga* Large Area Proportional Counters (LACs) is $\sim 4.0 \times 10^{-4}$ photons cm^{-2} s^{-1} per LAC beam of $1^\circ \times 2^\circ$, with the large beam oriented perpendicular to the Galactic plane (Yamauchi & Koyama 1993). Therefore, this implies a flux around 1.8×10^{-4} photons cm^{-2} s^{-1} per 0.9 deg^2, compatible with our individual measurements and slightly above the average value we have obtained. Moreover, we have performed an analysis of the slew data (when *RXTE* was pointing off the source) along the 4 days of observation and found marginal evidence of the presence of a line (3 σ) with a flux similar to that obtained from the on-source data. Although the slew data have been difficult to model and we had to restrict the energy range to 3.0–10 keV, we have fitted the data first to a bremsstrahlung, obtaining a reduced χ^2 of 2, and afterward to a bremsstrahlung plus a Gaussian line, improving the reduced χ^2 value down to 1. The above facts seem to rule out the possibility that the line comes from the source, although a deep observation by an instrument with imaging capabilities, if possible around periastron passage when the flux is higher, is still required to definitively solve this question.

4. DISCUSSION

4.1. *Orbital X-Ray Variability*

The *RXTE* observations presented here show evidence of flux variability occurring on timescales of days that is anticorrelated to the photon index of the spectrum. Since this happens while no changes are detected in the companion star and the maximum X-ray flux occurs near periastron, we propose that this variability is related to the orbital motion of the compact object accreting from the companion star wind along an eccentric orbit. Actually, the emission peak seems to take place at phase 0.8, not right at periastron passage. Leahy (2002) models a similar X-ray light curve observed in GX 301$-$2 through a non–spherically symmetric stellar wind accreted by the compact object following Bondi-Hoyle accretion.

We can consider that the wind of the companion star follows a β law and use a simple spherically symmetric Bondi-Hoyle accretion model (see Reig et al. 2003b for details) to study the ratio of maximum to minimum flux, to be compared to the observed one. For this purpose, we have assumed the following parameters: $M_{\rm opt} = 40\,M_\odot$, $R_{\rm opt} = 10\,R_\odot$, $\dot{M}_{\rm opt} = 1 \times 10^{-7}\,M_\odot$ yr^{-1} (average between the value given in Kudritzki & Puls [2000] from the wind-momentum relationship and the value inferred from optical spectroscopy by McSwain et al. [2004]), $v_\infty = 2440$ km s^{-1} (from observations by McSwain et al. 2004), $\beta = 0.8$, and finally a compact object of $M_{\rm X} = 1.4\,M_\odot$ with a radius of $R_{\rm X} = 15$ km in an eccentric orbit with $P_{\rm orb} = 3.9060$ days and $e = 0.35$ (Casares et al. 2005). These parameters provide an expected variability with a ratio of $\sim$10 between the maximum and minimum flux. Even when considering the uncertainties in all the involved parameters, ratios between 8 and 17 are found. These ratios are much lower than the variability ratio of $\sim$40 considering the previous eccentricity value of about 0.5 (McSwain et al. 2004), but still too large to explain the ratio of $\sim$2.5 observed by *RXTE*.

A possible solution that would easily reconcile the theoretical and the observed flux ratio is the presence of an accretion disk around the compact object. This would smooth the accretion rate of the compact object, implying lower and longer emission bumps around periastron passage in the light curves. Therefore, the difference between the expected and the observed flux ratio could be the first hint, in the X-ray domain and independent of the presence of relativistic jets, of the existence of an accretion disk in LS 5039, although it is not clear what kind of disk can be present at such a low ratio of X-ray to Eddington luminosity. It should be noted that for the short-timescale variations or miniflares, although they present the same flux–photon index anticorrelation as the rest of the observations suggested to be intrinsic to the source, the disk smoothing might not operate in the same manner as for long-lasting peaks, since it is the wind itself that changes rapidly. This could affect the accretion process in a more violent manner (e.g., inducing unsteady accretion and subsequent sudden X-ray flux increase) than a slow-changing flow, as would be the case for an approximately constant mass-loss rate.

BeppoSAX observations show a decrease in flux of about 50% between the periastron passage at phase 0.0 and the end of

the observations at phase 0.21 (Fig. 1 of Reig et al. 2003b). Interestingly, this is not too far from the flux reduction in this phase interval predicted by the accretion model discussed above, and we remind the reader that *BeppoSAX* had imaging capabilities, preventing the influence of background sources in the data. We note that the position of the maximum of emission in the *BeppoSAX* observations is consistent with being before periastron, as in the observations presented here. Therefore, these observations are complementary to the *RXTE* ones reported here and give clear support to the orbital variability being due to the eccentric orbit.

Concerning the long-term correlations in the X-ray emission and the stellar mass-loss rate, the new values for the equivalent width of the Hα absorption line of $\sim$2.8 Å (Casares et al. 2005) are similar to those obtained during the epochs when *ASCA* and *Chandra* observed the source. Moreover, taking into account the diffuse background emission, the average X-ray flux truly coming from the source during our observations is about 2×10^{-11} ergs cm^{-2} s^{-1}, similar also to the fluxes observed during *ASCA* and *Chandra* observations. Therefore, the apparent correlation between changes in the mass-loss rate of the stellar companion and the X-ray emission, suggested by Reig et al. (2003b) and supported by McSwain et al. (2004), seems to be confirmed by these new spectroscopic and X-ray results.

4.2. *Proposed Origin for the X-Ray Emission*

A signature of the existence of an accretion disk around the compact object is not present in any of the obtained X-ray spectra of the source, and no cutoff is present in data up to 30 keV. Actually, the possible detection of LS 5039 by instruments working in the energy range beyond the *RXTE* one (Burst and Transient Source Experiment [BATSE], Harmon et al. 2004; Imaging Compton Telescope [COMPTEL], Strong et al. 2001; EGRET, Paredes et al. 2000) seems to preclude the existence of any cutoff at energies beyond the *RXTE* range, typical of the thermal Comptonization spectra for emission produced in a corona. Therefore, we propose that the X-ray emission is due to inverse Compton (IC) and/or synchrotron processes within the relativistic jets of LS 5039. In our scenario, an increase in the accretion rate would imply a higher electron acceleration efficiency in the jets, filling with fresh particles the higher energy range of the electron energy distribution. This would harden the X-ray spectrum, which is actually observed by *RXTE* through the flux–photon index anticorrelation. The smooth evolution of the flux could be explained mainly, as mentioned above, by the dynamical timescales of a faint underlying accretion disk, which would smooth the emission variation around the periastron passage. It has been considered by several authors that relativistic electrons in the jet of a microquasar could produce significant X-ray emission by IC upscattering of the stellar photons or their own synchrotron photons (see Kaufman Bernadó et al. 2002; Georganopoulos et al. 2002; Reig et al. 2003a; Bosch-Ramon et al. 2005). Optically thin synchrotron radiation from a jet could also dominate at X-rays, depending on the matter density and magnetic field conditions within the jet (Markoff et al. 2001). Jet-dominated states could be common, and the disk radiation would appear covered by the nonthermal jet emission (Fender et al. 2003). These jet-dominated states are associated with the low-hard state of black hole X-ray binaries. The nature of the compact object in LS 5039 is not properly known yet. It could be a black hole (Casares et al. 2005), but its relatively high radio flux density and optically thin radio spectrum do not agree with the observed values found in black holes (Gallo et al. 2003). However, the observed X-ray spectrum is always very similar to the ones of black holes in the low-hard state: a power law with a photon index around 1.5 (see Tables 1 and 2).

5. SUMMARY

We have reported recent *RXTE* observations of LS 5039 covering a full orbital period of 4 days. The obtained results show moderate day-to-day variability that is interpreted as due to changes in the accretion rate because of the orbital motion of the compact object along an eccentric orbit, with an increase of emission right before periastron passage. In addition, the observed short-timescale flux variations (miniflares) are likely related to observed fast variations in the stellar wind properties. These observational results give support to the accretion scenario, making other possibilities like the young nonaccreting pulsar scenario (Martocchia et al. 2005) more unlikely. In parallel with the power-law flux variability, the flux of the iron line, detected at $\sim$6.7 keV as in previous *RXTE* observations, has remained constant within the errors and similar to the expected background line flux. Furthermore, slew data of these *RXTE* observations present marginal evidence of the iron line as well, and the line has not been detected by X-ray satellites with imaging capabilities. All these facts make us suggest that it is a background feature. No disk signatures are found in the spectra, although this is not rare for other X-ray binaries in the low-hard state. In fact, the presence of an accretion disk could explain the apparent smoothing of the flux changes along the orbit observed by *RXTE* with respect to what is predicted by using a Bondi-Hoyle accretion model. Finally, there appears to be an anticorrelation between the flux and the X-ray photon index along the orbit, reaching a maximum of emission and the hardest spectrum around phase 0.8. We suggest that a scenario in which the X-rays come from IC interactions and/or synchrotron emission within a relativistic jet could explain this anticorrelation, as well as the absence of a cutoff at hard X-rays. Although further theoretical work must be done, new observations to constrain the X-ray flux variability between periastron and apastron passages are necessary to better understand the orbital variability of LS 5039.

We thank the referee Jean Swank for relevant and valuable comments and suggestions that helped to improve the paper significantly. This research has made use of data obtained by the *RXTE* satellite. We are grateful to J. Casares and collaborators for allowing us to publish the new orbital ephemerides prior to their publication and for providing the equivalent width of Hα in contemporaneous spectroscopic observations. V. B.-R., J. M. P., M. R., and J. M. acknowledge partial support by Dirección General de Investigación (DGI) of the Spanish Ministerio de Educación y Ciencia (former Ministerio de Ciencia y Tecnología) under grants AYA-2001-3092, AYA-2004-07171-C02-01, and AYA-2004-07171-C02-02, as well as additional support from the European Regional Development Fund (ERDF/FEDER). During this work, V. B.-R. has been supported by the DGI of the Spanish Ministerio de Educación y Ciencia under the fellowship FP-2001-2699. M. R. acknowledges support by a Marie Curie Fellowship of the European Community programme Improving Human Potential under contract HPMF-CT-2002-02053.

REFERENCES

Bosch-Ramon, V., & Paredes, J. M. 2004, A&A, 417, 1075
Bosch-Ramon, V., Romero, G. E., & Paredes, J. M. 2005, A&A, 429, 267
Casares, J., Ribó, M., Paredes, J. M., Martí, J., Ribas, I., & Herrero, A. 2005, MNRAS, submitted
Clark, J. S., et al. 2001, A&A, 376, 476
Fender, R. P., Gallo, E., & Jonker, P. G. 2003, MNRAS, 343, L99
Gallo, E., Fender, R. P., & Pooley, G. G. 2003, MNRAS, 344, 60
Georganopoulos, M., Aharonian, F. A., & Kirk, J. G. 2002, A&A, 388, L25
Harmon, B. A., et al. 2004, ApJS, 154, 585
Hartman, R. C., et al. 1999, ApJS, 123, 79
Kaufman Bernadó, M. M., Romero, G. E., & Mirabel, I. F. 2002, A&A, 385, L10
Kudritzki, R., & Puls, J. 2000, ARA&A, 38, 613
Leahy, D. A. 2002, A&A, 391, 219
Markoff, S., Falcke, H., & Fender, R. 2001, A&A, 372, L25
Martí, J., Luque-Escamilla, P., Garrido, J. L., Paredes, J. M., & Zamanov, R. 2004, A&A, 418, 271
Martí, J., Paredes, J. M., & Ribó, M. 1998, A&A, 338, L71
Martocchia, A., Motch, C., & Negueruela, I. 2005, A&A, 430, 245
McSwain, M. V., Gies, D. R., Huang, W., Witta, P. J., Wingert, D. W., & Kaper, L. 2004, ApJ, 600, 927
McSwain, M. V., Gies, D. R., Riddle, R. L., Wang, Z., & Wingert, D. W. 2001, ApJ, 558, L43
Motch, C., Haberl, F., Dennerl, K., Pakull, M., & Janot-Pacheco, E. 1997, A&A, 323, 853
Paredes, J. M., Martí, J., Ribó, M., & Massi, M. 2000, Science, 288, 2340
Paredes, J. M., Ribó, M., Ros, E., Martí, J., & Massi, M. 2002, A&A, 393, L99
Predehl, P., & Schmitt, J. H. M. M. 1995, A&A, 293, 889
Reig, P., Kylafis, N. D., & Giannios, D. 2003a, A&A, 403, L15
Reig, P., Ribó, M., Paredes, J. M., & Martí, J. 2003b, A&A, 405, 285
Ribó, M. 2002, Ph.D. thesis, Univ. Barcelona
Ribó, M., Paredes, J. M., Romero, G. E., Benaglia, P., Martí, J., Fors, O., & García-Sánchez, J. 2002, A&A, 384, 954
Ribó, M., Reig, P., Martí, J., & Paredes, J. M. 1999, A&A, 347, 518
Strong, A. W., et al. 2001, AIP Conf. Proc. 587, Gamma 2001: Gamma-Ray Astrophysics, ed. St. Ritz, N. Gehrels, & C. R. Shrader (Melville: AIP), 21
Torres, D. F., Romero, G. E., Combi, J. A., Benaglia, P., Andernach, H., & Punsly, B. 2001, A&A, 370, 468
Valinia, A., & Marshall, F. E. 1998, ApJ, 505, 134
White, N. E., & Swank, J. H. 1984, ApJ, 287, 856
Yamauchi, S., & Koyama, K. 1993, ApJ, 404, 620